Multi-magnon excitations in Heisenberg spin- *S* chains with next-nearest-neighbour interactions

1996 J. Phys.: Condens. Matter 8 4781

(http://iopscience.iop.org/0953-8984/8/26/010)

J. Phys.: Condens. Matter **8** (1996) 4781–4795. Printed in the UK

Multi-magnon excitations in Heisenberg spin-S chains with next-nearest-neighbour interactions

S L M Cyr†, B W Southern†§ and D A Lavis‡

† Department of Physics, University of Manitoba, Winnipeg, Manitoba, Canada R3T 2N2
‡ Department of Mathematics, King's College, The Strand, London WC2R 2LS, UK

Received 12 March 1996

Abstract. The spectra of both two- and three-magnon excitations in Heisenberg spin chains with next-nearest-neighbour (NNN) interactions are studied using scaling methods and the recursion method respectively. Both two-spin and three-spin couplings are considered for general spin S. In the three-magnon case, the asymptotic behaviour of the recursion coefficients can be used to directly identify the presence of bound states in the spectrum. Both integrable and non-integrable models can be studied, and the integrable models display special features in the bound-state spectra. Our results for the three-magnon bound states of $S = 1$ chains differ appreciably from those obtained in previous studies based upon an integral equation approach.

1. Introduction

The *multi*-magnon spectrum of generalized spin-S Heisenberg chains with nearest-neighbour interactions has recently been studied using the recursion method [1, 2]. The approach involved expressing the m-magnon Schrödinger equation in a tight-binding form which takes the form of a semi-infinite chain for the two-magnon case [3] and a semi-infinite triangular net for the three-magnon problem. In the latter case, the recursion method was used to transform this net to a semi-infinite inhomogeneous chain, and the resulting tridiagonal form could then be used to provide a continued-fraction representation of the density of states. The spectrum of the general Hamiltonian consists of bound states and two distinct types of scattering state. These latter solutions correspond to excitations propagating in the bulk or along the surface of the triangular net whereas the bound states are localized states. Special features of the bound states were associated with integrable cases of the general model. Bethe [4] first showed how to obtain the eigenvalues and eigenvectors of the $S = 1/2$ Heisenberg chain using a method which is now called the Bethe *ansatz*. However, this method of solution can only be used for the integrable models [5–10]. When the spin $S \neq \frac{1}{2}$ or second-neighbour interactions are added, the model is no longer integrable and the Bethe *ansatz* cannot be used. Tsvelik [11] has considered an $S = 1/2$ model with both nearest-neighbour interactions and a second-neighbour three-spin coupling. This model remains integrable for all values of the couplings but is not integrable for $S > \frac{1}{2}$. Grabowski and Mathieu [12] have constructed all the quantum integrals of motion for the isotropic Heisenberg $S = 1/2$ chain, and the model with NNN two-spin interactions is integrable if a four-spin term is also included.

§ To whom any correspondence should be addressed.

0953-8984/96/264781+15$19.50

In the case of a ferromagnetic ground state, the one-magnon and two-magnon problems can be solved exactly [13] for any range of interaction using a variety of methods. However, there have been very few papers which have considered multi-magnon excitations in systems with NNN interactions. The two-magnon spectrum with second-neighbour interactions has been investigated for the $S = 1/2$ Heisenberg Hamiltonian [14–18] using both analytic and numerical methods. Bound states exist both below and above the scattering-state continuum. Kadolkar *et al* [19] have recently studied the three-magnon spectrum of the $S = 1$ Heisenberg model with NNN interactions. Their method is based upon the integral equation approach used by Millet and Kaplan [20]. However, the method seems to produce spurious solutions as was also the case for $S = 1/2$ in the work of Millet and Kaplan.

In the present work we describe a different method for calculating three-magnon excitations in ferromagnets with NNN interactions [21]. Our approach to the three-magnon problem maps it exactly onto an effective tight-binding Hamiltonian. In the next section we outline our method of solution, and our results for the multi-magnon excitation spectrum of various spin-S models are given in section 3.

2. The model

We consider the following Hamiltonian with interactions beyond nearest neighbours:

$$\widehat{\mathcal{H}} = -J_1 \sum_i \widetilde{\boldsymbol{S}}_i \cdot \widetilde{\boldsymbol{S}}_{i+1} - J_2 \sum_i \widetilde{\boldsymbol{S}}_i \cdot \widetilde{\boldsymbol{S}}_{i+2} - J_3 \sum_{i=1}^{N} \widetilde{\boldsymbol{S}}_{i-1} \cdot (\widetilde{\boldsymbol{S}}_i \times \widetilde{\boldsymbol{S}}_{i+1}) \qquad (1)$$

where the $\widetilde{\boldsymbol{S}}_i$ are quantum spins located at the sites of a uniform chain with lattice spacing a. The ferromagnetic state with all N spins parallel is an exact eigenstate of (1) with energy $E_0 = -(J_1 + J_2)NS^2$. We shall study the excitation spectrum of (1) relative to this ferromagnetic state.

The one-magnon excitation energy is given by

$$E_1 = (2SJ_1 + 4S^2 J_3 \sin ka)(1 - \cos ka) + 2SJ_2(1 - \cos 2ka) \qquad (2)$$

where k is a wavevector in the range $-\pi/a \leqslant k \leqslant \pi/a$. In order for the second-neighbour couplings not to frustrate the system, we have restrictions on the allowed values of the dimensionless ratios $\beta = J_2/J_1$ and $\gamma = 2S|J_3|/J_1$. We assume $J_1 > 0$, and the condition that $E_1 \geqslant 0$ is equivalent to $1 + 2\beta + \mathrm{sign}(\beta)\sqrt{4\beta^2 + \gamma^2} \geqslant 0$ if $\beta \neq 0$, or $\gamma \leqslant 1$ if $\beta = 0$. For the case $\gamma = 0$, the former condition reduces to $\beta \geqslant -\frac{1}{4}$.

2.1. Two-magnon excitations

In general, the two-magnon problem is soluble in any dimension, since it reduces to essentially a defect problem on a d-dimensional lattice. For $d = 1$ Majumdar [14] has studied the Hamiltonian (1) with $J_3 = 0$ for $S = \frac{1}{2}$, and Bahurmuz and Loly [17] have studied the same problem for both $S = 1$ and $S = \frac{1}{2}$. We will extend these studies of the two-magnon problem to the general case of J_3 non-zero and for general S.

The two-magnon excitations are solutions of the Schrödinger equation which can be written in terms of the basis of two-spin deviation states

$$|i, j\rangle = S_i^+ S_j^+ |0\rangle \qquad (i \leqslant j). \qquad (3)$$

where $|0\rangle$ represents the ferromagnetic state with all spins aligned in the negative z-direction. Using the translational invariance of the Hamiltonian, we transform to a mixed orthonormal basis $|K; r\rangle$, where K represents the total wavevector of the pair and $r = |j - i|$ represents

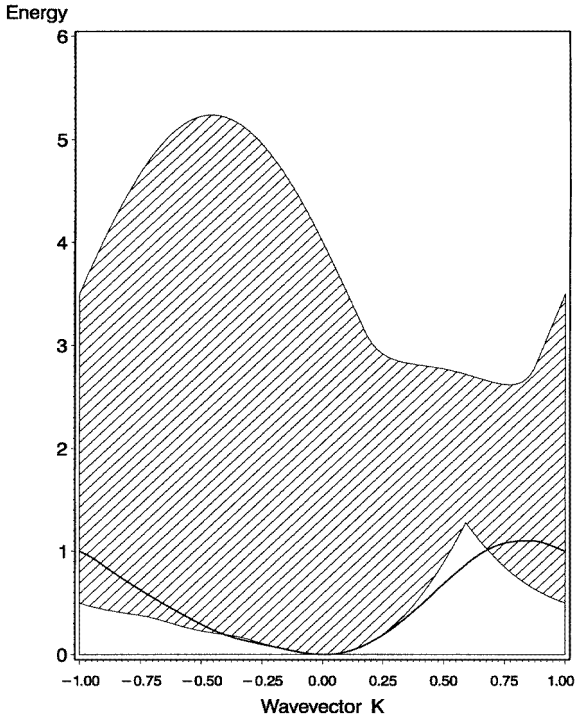

Figure 1. The two-magnon excitation spectrum showing the bound-state branch (solid line) and the scattering-state continuum (shaded region) for the $S = \frac{1}{2}$ Tsvelik model with $\gamma = \frac{3}{4}$. The energy is in units of $2SJ_1$ and the wavevector K is in units of π/a.

the relative separation of the spin deviations. In this mixed basis, the Schrödinger equation for the amplitudes c_r has a tight-binding form:

$$\left.\begin{aligned}
&(E-\varepsilon_0)c_0 = V_0c_1 + V_0'c_2 \\
&(E-\varepsilon_1)c_1 = V_0c_0 + V_1c_2 + V'c_3 \\
&(E-\varepsilon_2)c_2 = V_0'c_0 + V_1c_1 + Vc_3 + V'c_4 \\
&(E-\varepsilon\ )c_r = V'c_{r-2} + Vc_{r-1} + Vc_{r+1} + V'c_{r+2} \qquad (r>2)
\end{aligned}\right\} \tag{4}$$

where the tight-binding parameters are given by

$$\left.\begin{aligned}
\varepsilon_0 &= 4S(J_1+J_2) \\
\varepsilon_1 &= (4S-1)J_1 + 2SJ_2(2-\cos K) + 2SJ_3(1-S)\sin K \\
\varepsilon_2 &= 4SJ_1 + (4S-1)J_2 \\
\varepsilon\ &= 4SJ_1 + 4SJ_2 \\
V_0 &= -2\sqrt{S\,(2S-1)}J_1\cos\frac{K}{2} + 4SJ_3\sqrt{S\,(2S-1)}\sin\frac{K}{2} \\
V_0' &= -2\sqrt{S\,(2S-1)}J_2\cos K - 2SJ_3\sqrt{S\,(2S-1)}\sin K \\
V_1 &= -2SJ_1\cos\frac{K}{2} + 2S(2S-1)J_3\sin\frac{K}{2} \\
V\ &= -2SJ_1\cos\frac{K}{2} + 4S^2J_3\sin\frac{K}{2} \\
V' &= -2SJ_2\cos K - 2S^2J_3\sin K.
\end{aligned}\right\} \tag{5}$$

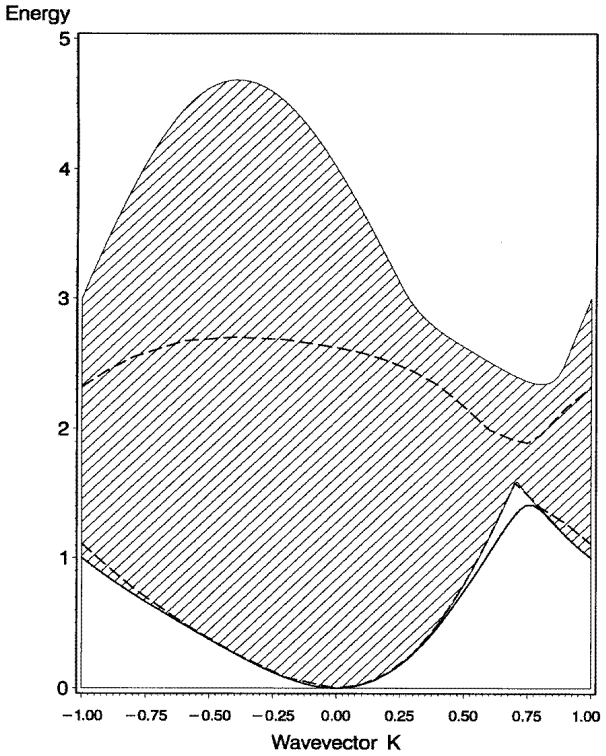

Figure 2. The two-magnon excitation spectrum showing the bound-state branch (solid line), the scattering-state continuum (shaded region) and the resonances (dashed lines) for the $S = 1$ Tsvelik model with $\gamma = \frac{1}{2}$. The energy is in units of $2SJ_1$ and the wavevector K is in units of π/a.

Equations (4) and (5) describe interactions between two magnons, and the bound-state solutions can be obtained using a real-space rescaling method [3]. The basic idea of the method is to perform a transformation on the equations which eliminates a fraction of the degrees of freedom but leaves the equations invariant in form with renormalized parameters. At certain values of S, K, β and γ, the equations in (4) reduce to a nearest-neighbour problem, and analytic results for the bound-state energies can be obtained using the expressions in [3]. However, in general both nearest- and next-nearest-neighbour interactions are present. Using site 0 as a reference, the amplitudes $c_1, c_2, \ldots, c_{b-1}$ can be eliminated from (4) to obtain the rescaled equations

$$\left.\begin{aligned}
(E-\tilde{\varepsilon}_0)c_0 &= \tilde{V}_0 c_b + \tilde{V}_0' c_{2b} \\
(E-\tilde{\varepsilon}_1)c_b &= \tilde{V}_0 c_0 + \tilde{V}_1 c_{2b} + \tilde{V}' c_{3b} \\
(E-\tilde{\varepsilon}_2)c_{2b} &= \tilde{V}_0' c_0 + \tilde{V}_1 c_b + \tilde{V} c_{3b} + \tilde{V}' c_{4b} \\
(E-\tilde{\varepsilon}\ )c_r &= \tilde{V}' c_{r-2b} + \tilde{V} c_{r-b} + \tilde{V} c_{r+b} + \tilde{V}' c_{r+2b} \qquad r > 2b
\end{aligned}\right\} \tag{6}$$

which now involve only the amplitudes $c_0, c_b, c_{2b}, \ldots$ for some integer $b > 1$. The forms for the rescaled (tilded) parameters in terms of the original parameters are quite complicated and will be published separately [22]. They depend on the choice of b, but in the limit $b \to \infty$ all interactions approach zero and then any states with $c_0 \neq 0$ correspond to $E = \tilde{\varepsilon}_0$. The same method can also be applied to any of the other coefficients c_i in (4).

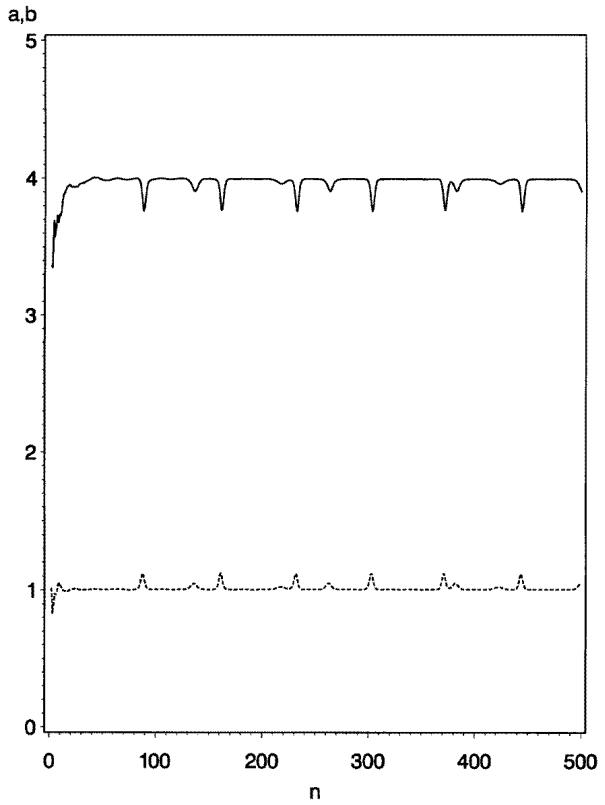

Figure 3. The recursion coefficients a_n (solid curve) and b_n (dashed curve) as a function of the index n in the case where $S = 1$, $K = \pi/a$, $\beta = 0.18$ and $\gamma = 0$.

Using this approach the spectral properties of the two-magnon excitations can be found for any values of K, S, β and γ. Our results for cases with $\beta \neq 0, \gamma = 0$ agree with the previous work cited above. We simply illustrate here some typical spectra for cases with $\gamma \neq 0$. Figure 1 shows the excitation spectrum for the $S = 1/2$ model with $\beta = 0$ and $\gamma = 3/4$. This is an integrable model for all values of γ, and the bound state can enter the continuum of scattering states without broadening into a resonance. Figure 2 shows the excitation spectrum for $S = 1, \beta = 0$ and $\gamma = 1/2$. This model is no longer integrable and the bound state now broadens into a resonance when it enters the continuum. These features are important differences between integrable and non-integrable spin models and can be used as a means of identifying integrable cases.

The information about the two-magnon spectrum will be used below to describe the scattering-state solutions of the three-magnon excitations.

2.2. Three-magnon excitations

The three-magnon excitations are solutions of the Schrödinger equation, which can be written in the basis of three-spin deviation states:

$$|r, l, m\rangle = S_r^+ S_l^+ S_m^+ |0\rangle \qquad (r \leqslant l \leqslant m). \tag{7}$$

Using centre-of-mass and relative coordinates for the sites r, l and m, we can express the Hamiltonian in a mixed orthonormal basis $|K; x, y\rangle$, where K represents the total wavevector of the three-magnon state and $x = |l - r|$ and $y = |m - l|$ represent the relative separation of the spin deviations in units of the lattice spacing a. In this mixed basis the Schrödinger equation for the ket amplitudes c_{xy} can be expressed in the following tight-binding form:

$$(E - \varepsilon_{xy})c_{xy} = \sum_{i,j} A_{ij}^{xy} c_{x+i,y+j} \tag{8}$$

where the right-hand side generally involves twelve terms. The coefficients ε_{xy} and A_{ij}^{xy} are defined in table 1. The relationships between these tight-binding parameters and the Hamiltonian are given in table 2. The parameters are complex functions of the total momentum K of the three-magnon state. In table 1, U^* represents the complex conjugate of U and in table 2 the variable $\zeta = \mathrm{e}^{\mathrm{i}Ka/3}$.

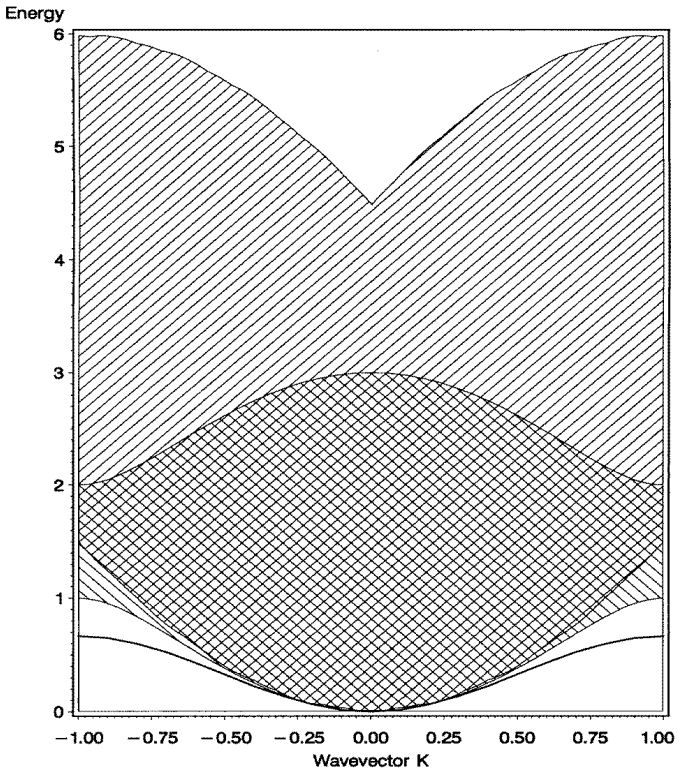

Figure 4. The three-magnon spectrum of the $S = \frac{1}{2}, \beta = 0, \gamma = 0$ Heisenberg model with energy in units of $2SJ_1$ and K in units of π/a. The shaded areas represent the two overlapping scattering-state continua and the solid line below the continua indicates a bound state.

The system of equations (8) corresponds to a semi-infinite triangular lattice with a surface along the positive x- and y-axes. The $x = 0, y = 0$ surfaces describe states where two deviations are on the same site and the origin corresponds to the state with three deviations on the same site. In general, a site (x, y) interacts with six nearest neighbours (denoted by the unprimed Us) and with six next-nearest neighbours (denoted by the primed Us).

Table 1. Coefficients for the three-magnon equations ($r, s > 2$).

		$A^{xy}_{i,j}$											
x, y	ε_{xy}	$-1,0$	$0,1$	$1,-1$	$1,0$	$0,-1$	$-1,1$	$-2,0$	$0,2$	$2,-2$	$2,0$	$0,-2$	$-2,2$
$0,0$	ε_{00}	0	U_0	0	U_0^*	0	0	0	$U_0^{'}$	0	$U_0^{'*}$	0	0
$0,1$	ε_{01}	0	U_3	U_1	U_2^*	U_0^*	0	0	$U_3^{'}$	0	$U_2^{'*}$	0	0
$1,0$	ε_{01}	U_0	U_2	0	U_3^*	0	U_1^*	0	$U_2^{'}$	0	$U_3^{'*}$	0	0
$1,1$	ε_{11}	U_2	U_5	U_4	U_5^*	U_2^*	U_4^*	0	$U^{'}$	0	$U^{'*}$	0	0
$0,2$	ε_{02}	0	U_7	U_4	U_8^*	U_3^*	0	0	$U_3^{'}$	$U_1^{'}$	$U_2^{'*}$	$U_0^{'*}$	0
$2,0$	ε_{02}	U_3	U_8	0	U_7^*	0	U_4^*	$U_0^{'}$	$U_2^{'}$	0	$U_3^{'*}$	0	$U_1^{'*}$
$1,2$	ε_{12}	U_8	U_9	U_6	U_{10}^*	U_5^*	U_8^*	0	$U^{'}$	$U_2^{'}$	$U^{'*}$	$U_2^{'*}$	0
$2,1$	ε_{12}	U_5	U_{10}	U_8	U_9^*	U_8^*	U_6^*	$U_2^{'}$	$U^{'}$	0	$U^{'*}$	0	$U_2^{'*}$
$2,2$	ε_{02}	U_{10}	U	U_{10}	U^*	U_{10}^*	U_{10}^*	$U_2^{'}$	$U^{'}$	$U_2^{'}$	$U^{'*}$	$U_2^{'*}$	$U_2^{'*}$
$0,s$	ε_{00}	0	U_7	U_8	U_8^*	U_7^*	0	0	$U_3^{'}$	$U_2^{'}$	$U_2^{'*}$	$U_3^{'*}$	0
$r,0$	ε_{00}	U_7	U_8	0	U_7^*	0	U_8^*	$U_3^{'}$	$U_2^{'}$	0	$U_3^{'*}$	0	$U_2^{'*}$
$1,s$	ε_{1s}	U_8	U_9	U_{10}	U_{10}^*	U_9^*	U_8^*	0	$U^{'}$	$U^{'}$	$U^{'*}$	$U^{'*}$	0
$r,1$	ε_{1s}	U_9	U_{10}	U_8	U_9^*	U_8^*	U_{10}^*	$U^{'}$	$U^{'}$	0	$U^{'*}$	0	$U^{'*}$
$2,s$	ε_{2s}	U_{10}	U	U	U^*	U^*	U_{10}^*	$U_2^{'}$	$U^{'}$	$U^{'}$	$U^{'*}$	$U^{'*}$	$U_2^{'*}$
$r,2$	ε_{2s}	U	U	U_{10}	U^*	U_{10}^*	U^*	$U^{'}$	$U^{'}$	$U_2^{'}$	$U^{'*}$	$U_2^{'*}$	$U^{'*}$
r,s	ε_{00}	U	U	U	U^*	U^*	U^*	$U^{'}$	$U^{'}$	$U^{'}$	$U^{'*}$	$U^{'*}$	$U^{'*}$

In order to obtain information about the spectral properties of the general Hamiltonian in (1), we have used the recursion method [23] to transform this triangular system to a semi-infinite chain. This provides a continued-fraction representation of the local Green's function which can easily be used to calculate the local density of states. The method is based on a three-term recurrence relation of the form

$$\widehat{\mathcal{H}}|u_n\rangle = b_n|u_{n-1}\rangle + a_n|u_n\rangle + b_{n+1}|u_{n+1}\rangle \tag{9}$$

where $a_n, b_n \in \mathcal{R}$ and $|u_n\rangle$ is the nth state of an arbitrary complete orthonormal set of states. To start the procedure we define $|u_{-1}\rangle \equiv 0$ and choose some arbitrary normalized member $|u_0\rangle$ of the three-magnon basis. Then, from (9), $|u_1\rangle$ is given by

$$b_1|u_1\rangle = \widehat{\mathcal{H}}|u_0\rangle - a_0|u_0\rangle \tag{10}$$

with

$$a_0 = \langle u_0|\widehat{\mathcal{H}}|u_0\rangle \qquad b_1^2 = \langle u_0|\widehat{\mathcal{H}}^2|u_0\rangle - a_0^2. \tag{11}$$

Once we have the first two states we can use (9) to generate the rest. We have

$$b_{n+1}|u_{n+1}\rangle = \widehat{\mathcal{H}}|u_n\rangle - b_n|u_{n-1}\rangle - a_n|u_n\rangle \tag{12}$$

where

$$a_n = \langle u_n|\widehat{\mathcal{H}}|u_n\rangle \qquad b_{n+1}^2 = \langle u_n|\widehat{\mathcal{H}}^2|u_n\rangle - a_n^2 - b_n^2. \tag{13}$$

By iterating this procedure the set of states $\{|u_n\rangle\}$ can be found which will transform the Hamiltonian to the desired canonical form, and the resulting tridiagonal matrix will contain

Table 2. Three-magnon tight-binding parameters.

ε_{00}	$6S(J_1+J_2)$
ε_{01}	$\varepsilon_{00}-2J_1$
ε_{11}	$\varepsilon_{00}-2J_1-J_2$
ε_{02}	$\varepsilon_{00}-2J_2$
ε_{12}	$\varepsilon_{00}-J_1-J_2$
ε_{1s}	$\varepsilon_{00}-J_1$
ε_{2s}	$\varepsilon_{00}-J_2$
U	$-\zeta SJ_1-2\mathrm{i}\zeta S^2J_3$
U_0	$-\zeta\sqrt{3S(S-1)}(J_1+2\mathrm{i}SJ_3)$
U_1	$-\zeta(2S-1)J_1-\zeta^*SJ_2-2\mathrm{i}S(2S-1)\zeta J_3-\mathrm{i}S(2-S)\zeta^2J_3$
U_2	$-\zeta\sqrt{S(2S-1)}J_1-\zeta^*\sqrt{S(2S-1)}J_2-\mathrm{i}S\sqrt{S(2S-1)}\zeta J_3$ $-\mathrm{i}(S-1)\sqrt{S(2S-1)}\zeta J_3-\mathrm{i}(S-1)\sqrt{S(2S-1)}\zeta^2J_3$
U_3	$-\zeta SJ_1-\mathrm{i}S^2\zeta J_3+\mathrm{i}S(2-S)\zeta J_3$
U_4	$-\zeta\sqrt{S(2S-1)}(J_1+\mathrm{i}SJ_3+\mathrm{i}(S-1)J_3)$
U_5	$-\zeta SJ_1-\zeta^*SJ_2-\mathrm{i}S^2\zeta J_3-\mathrm{i}S(S-1)\zeta J_3$ $-\mathrm{i}S(S-1)\zeta^2J_3$
U_6	$-\zeta SJ_1-2\mathrm{i}S(S-1)\zeta J_3$
U_7	$-\zeta SJ_1-2\mathrm{i}S^2\zeta J_3$
U_8	$-\zeta\sqrt{S(2S-1)}(J_1+2\mathrm{i}SJ_3)$
U_9	$-\zeta SJ_1-\zeta^*SJ_2-2\mathrm{i}S^2\zeta J_3-\mathrm{i}S(S-1)\zeta^2J_3$
U_{10}	$-\zeta SJ_1-\mathrm{i}S^2\zeta J_3-\mathrm{i}S(S-1)\zeta J_3$
U'	$-\zeta SJ_2+\mathrm{i}S^2\zeta^2J_3$
U_0'	$-\zeta\sqrt{3S(S-1)}J_2+\mathrm{i}S\sqrt{3S(S-1)}\zeta^2J_3$
U_1'	$-\zeta(2S-1)J_2-\mathrm{i}S(2S-1)\zeta^2J_3$
U_2'	$-\zeta\sqrt{S(2S-1)}J_2+\mathrm{i}S\sqrt{S(2S-1)}\zeta^2J_3$
U_3'	$-\zeta SJ_2+\mathrm{i}S^2\zeta^2J_3$

the a_n and b_n as its elements. In the new basis the Hamiltonian satisfies

$$\widehat{\mathcal{H}}\begin{pmatrix}|u_0\rangle\\|u_1\rangle\\|u_2\rangle\\\vdots\end{pmatrix}=\begin{bmatrix}a_0&b_1&&&\\b_1&a_1&b_2&&0\\&b_2&a_2&b_3&\\&&0&&\ddots\end{bmatrix}\begin{pmatrix}|u_0\rangle\\|u_1\rangle\\|u_2\rangle\\\vdots\end{pmatrix}\tag{14}$$

and corresponds to an inhomogeneous nearest-neighbour tight-binding chain. The precise values of the a_n and b_n generated will depend upon the choice of initial ket.

For the infinite system of equations represented by (8), the recursion process continues indefinitely and this raises the question of when and how to stop the procedure. There are a number of possibilities [24, 25, 26] for the behaviour of the a_n- and b_n-coefficients as a function of n. The coefficients may approach constants, approach some kind of periodic oscillation or behave in a more complicated fashion. The asymptotic form for the coefficients is determined by the scattering states of the spectrum. If these states are composed of overlapping continua with no gaps, then the coefficients approach constant values which are

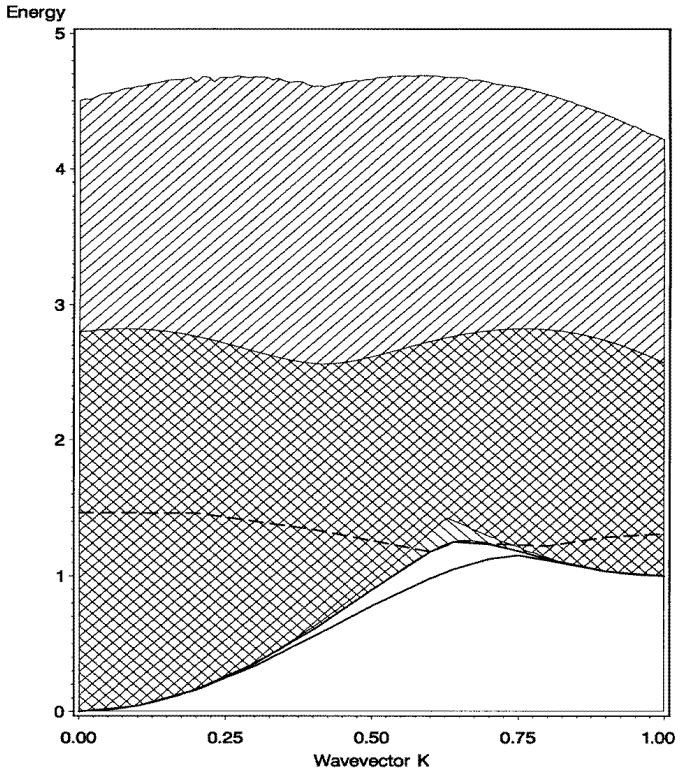

Figure 5. The three-magnon spectrum of the $S = \frac{1}{2}, \beta = 1$ Heisenberg case with energy in units of $2SJ_1(1+\beta)$ and K in units of π/a. The shaded areas represent the two overlapping scattering-state continua, the solid lines below the continua indicate the bound states and the dashed line indicates a resonance.

determined by the maximum and minimum values of the overlapping continua as follows:

$$\begin{aligned} a &\to (E_{\max} + E_{\min})/2 \\ b &\to (E_{\max} - E_{\min})/4. \end{aligned} \tag{15}$$

For the three-magnon case, these continua have energies equal to either the sum of three free magnons or two bound and one free. For $S > 1/2$ there can be more than one two-magnon bound-state branch and there is a continuum corresponding to each branch. If the superposition of the continua leads to internal gaps in the continuum, then the asymptotic form of the coefficients can be more complicated [26] and will depend upon the values of the energies at the edges of the gaps as well. In each case, once the asymptotic behaviour is reached, the iteration process can be terminated and the remaining coefficients can be obtained using the asymptotic form. In our case, knowledge of the complete two-magnon spectrum is all that is required to predict this behaviour.

The local density of states corresponding to the initial ket u_0 can be obtained directly from the continued-fraction representation of the Green's function in terms of the coefficients a_n and b_n. The information about both the one- and two-magnon spectra allows the regions of the three-magnon continua to be easily identified. The three-magnon density of states can then be used to identify the location of bound states. Each set of coefficients is calculated at a fixed value of K and the information obtained in this way can then be combined to

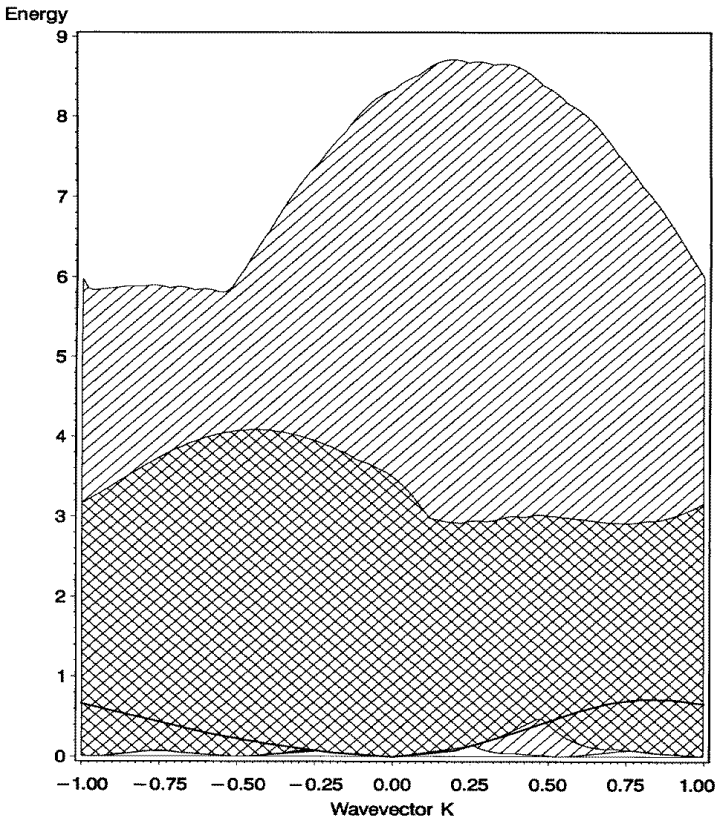

Figure 6. The three-magnon spectrum of the $S = \frac{1}{2}$, $\gamma = 1$ integrable model with energy in units of $2SJ_1$ and K in units of π/a. The shaded areas represent the two overlapping scattering-state continua and the solid line indicates the bound state.

show the dispersion curve for the bound-state branches. The method can be applied to the general Hamiltonian in (1) as it does not require the model to be integrable.

Southern *et al* [1] have shown that the presence of bound states can also be detected from the behaviour of the coefficients in the asymptotic region. Figure 3 shows an example of the recursion coefficients obtained for the case where $S = 1$, $K = \pi/a$, $\beta = 0.18$ and $\gamma = 0$. The coefficients appear to approach constant values consistent with the minimum and maximum energies of the three-magnon continua as predicted from the one- and two-magnon solutions. However, there are pulse-like deviations from these values which occur periodically. These pulses are a direct result of a loss of orthogonality of the new basis states which is dependent upon the numerical precision used. The net effect is that the bound states become a narrow band with a width determined by this precision. The coefficients behave as if there is a gap between the continua and the bound states and the amplitude of the pulses is a direct measure of this gap. Hence the number of pulses and their amplitudes can be used to directly identify the presence and location of bound states outside the continua. The coefficients in figure 3 indicate the presence of two bound states below the continua.

In the following section we present the results of our calculations. We will only consider the cases with either $\beta = 0$ or $\gamma = 0$, but the spin magnitude S is arbitrary.

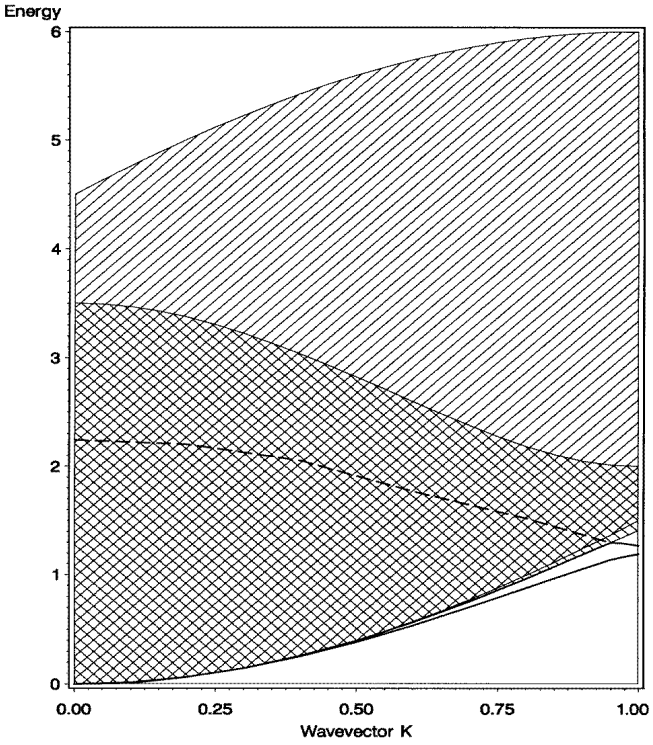

Figure 7. The three-magnon spectrum for the $S = 1, \beta = 0$ Heisenberg case with energy in units of $2SJ_1$ and K in units of π/a. The shaded areas represent the two overlapping scattering-state continua, the solid lines below the continua indicate the bound states, and the dashed line indicates the resonance.

3. Results

3.1. The $S = \frac{1}{2}$ Heisenberg case ($\gamma = 0$)

The three-magnon spectrum of the integrable $S = \frac{1}{2}$, $\beta = 0$ Heisenberg case is shown in figure 4 for the case where $\gamma = 0$. The shading slanted to the left indicates the two-bound–one-free-magnon continuum, the shading to the right indicates the three-free-magnons continuum and the cross-hatched region indicates where the two continua overlap. The solid line below the continua indicates a bound state. These results completely agree with those obtained by Bethe [4] using an *ansatz* for the three-particle wavefunction. If $\gamma \neq 0$, the model remains integrable but the excitation energies are no longer even functions of K. However, when $\gamma = 0$, we can restrict our consideration to positive values of K.

For negative values of β, the first- and second-neighbour couplings compete and the three-magnon energies all decrease, with an instability first occurring near $K = 0$ when $\beta < -\frac{1}{4}$. However, as β increases from zero, a resonance begins to appear inside the continuum and eventually emerges as an additional bound state below the continuum for a small range of β at intermediate values of K. The $\beta = 1$ case is shown in figure 5 where the second bound state is weakly bound in the region near $K = 0.65\pi/a$. As β increases further this upper bound state moves back inside the continuum. In the limit $\beta \to \infty$ we have a chain with only second-neighbour interactions and the model is again integrable.

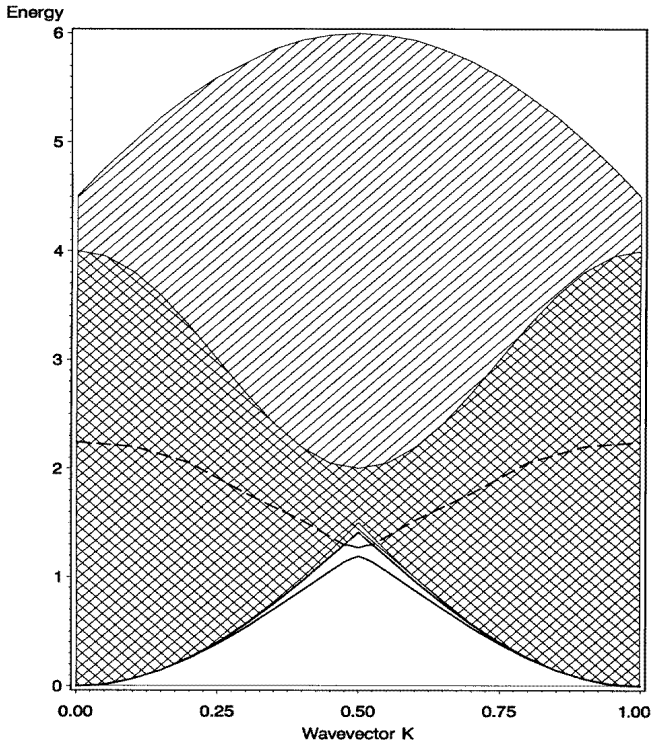

Figure 8. The three-magnon spectrum of the $S = 1, \beta \to \infty$ Heisenberg case with energy in units of $2SJ_1(1 + \beta)$ and K in units of π/a. The shaded areas represent the two overlapping scattering-state continua, the solid lines below the continua indicate the bound states and the dashed line indicates the resonance.

A characteristic property of integrable models is that the bound-state branches can pass through the continua without becoming resonances. Our results indicate that the spin-$\frac{1}{2}$ Heisenberg case is not integrable for $\beta \neq 0$.

3.2. The $S = \frac{1}{2}$ integrable case ($\beta = 0$)

When $\gamma \neq 0$, the three-spin coupling in (1) introduces an asymmetry between $\pm K$. Positive and negative values of γ both lead to competing effects and we can restrict our consideration to $\gamma \geqslant 0$. As γ increases from zero the lower continuum edge decreases in energy, with the bound state entering the continuum first near $K = \pm\pi/a$ and eventually for intermediate values of K. Figure 6 shows the spectrum where $\gamma = 1$. The bound states do not broaden into resonances inside the continua. These results confirm the general features of integrable models: bound states and scattering states can exist at the same energy but are completely decoupled. As one moves away from integrability, the bound states inside the continuum should broaden into resonances.

3.3. The $S = 1$ Heisenberg case ($\gamma = 0$)

The three-magnon results for the $S = 1$ Heisenberg case are shown in figure 7 for $\beta = 0$. This case was discussed in detail by Southern *et al* [1]. The shaded region is

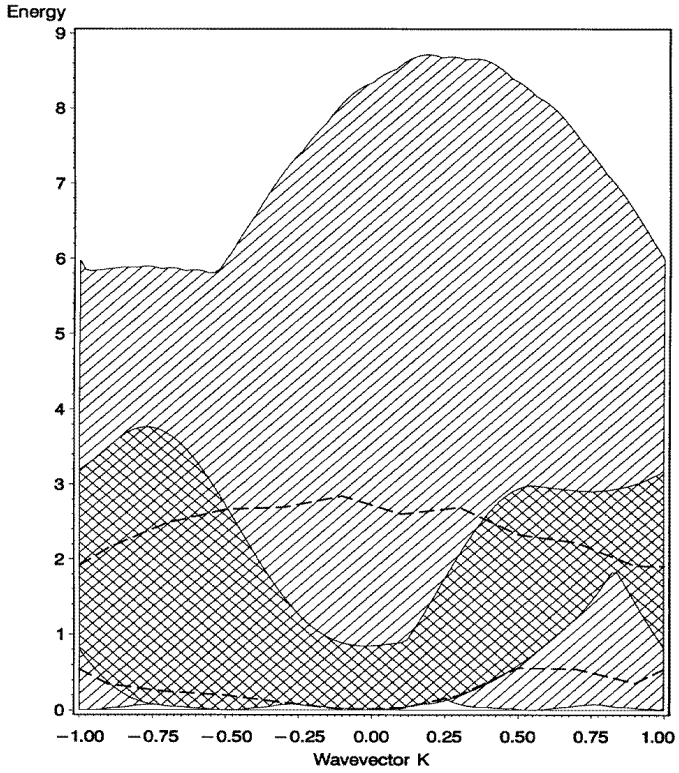

Figure 9. The three-magnon spectrum of the $S = 1$, $\gamma = 1$ NNN model with energy in units of $2SJ_1$ and K in units of π/a. The shaded areas represent the two overlapping scattering-state continua and the dashed lines indicate the resonances.

the scattering-state continuum (shading slanted to the left indicates the two-bound–one-free-magnon continuum, and shading slanted to the right indicates the three-free-magnons continuum), the solid lines below the continuum indicate the bound states, and the dashed line indicates a resonance. The energies of the bound states at $K = \pi/a$ agree fairly well with the energies found by Millet and Kaplan [20] and Kadolkar, Ghosh and Sarma [19] using an integral equation approach. We find two bound states below the continuum: the lower state exists across the entire Brillouin zone but the upper enters the continuum near $K = \pi/a$ and becomes a resonance. The energies of our lower bound-state branch agree with those of Kadolkar, Ghosh and Sarma, but they find that the upper bound state is present for all K-values in disagreement with our results. This difference may be due to their method of discretizing the integral equations with the result that the two-bound–one-free-magnon continuum may be indistinguishable from a true bound state.

Kadolkar *et al* did not consider the case of NNN interactions which compete with the nearest-neighbour terms. As β decreases from zero the lower continuum edge and the bound-state energies all decrease. For $\beta < -\frac{1}{4}$ the energies near $K = 0$ become negative.

As β increases from zero we find that the upper bound state's range of K decreases and eventually disappears at about $\beta \sim 0.21$. At a larger value of $\beta \sim 0.266$, the lower bound state begins to touch the continuum at $K = \pi/a$ but exists for all $0 < K < \pi/a$. As $\beta \to \infty$ (figure 8), the upper bound state emerges from the continuum at values of K

closer to $K = \pi/2a$, and we simply have the $\beta = 0$ case with the lattice distance doubled. These results do not agree with those reported previously by Kadolkar *et al* [19]. For all $\beta > 0$, we find that only the lower bound-state branch exists for all K. The upper branch is present near $K = \pi/a$ for small β and near $K = \pi/2a$ for large values of β. However, this upper branch always enters the scattering-state continuum and becomes a resonance.

3.4. The $S = 1$ NNN case ($\beta = 0$)

The $S = 1$, $\gamma = 0$ Heisenberg case, shown in figure 7, has two bound states near $K = \pm\pi/a$. The upper bound state enters the continuum near $K = \pm 0.9\pi/a$ and becomes a resonance, and the lower bound state exists for all values of $K \neq 0$. As γ increases the upper state completely enters the continuum and becomes a resonance for all values of K. The lower bound state enters the continuum near $K = \pm\pi/a$ and also becomes a resonance. This behaviour differs from that in the $S = \frac{1}{2}$ case and is due to the non-integrability of the $S = 1$ model. When γ is increased to one (figure 9), the lower bound state has completely entered the continuum, so there are two resonances inside the continuum. As the NNN term drives the ferromagnetic state towards instability, the bound states disappear.

4. Summary

We have studied the nature of both two-magnon and three-magnon excitations in spin-S Heisenberg chains with interactions which extend beyond nearest neighbours. In the two-magnon case, scaling methods can be used to extract general features of the spectrum including both bound and scattering states. For the three-magnon case, the recursion method can be used to study the complete spectrum. The termination of the continued fraction can be performed using the knowledge of the two-magnon spectrum. Special features of the excitations are associated with the integrable models.

Our results for the three-magnon excitations of the $S = 1$ Heisenberg model with second-neighbour interactions are different from those reported previously by Kadolkar *et al* [19]. We believe that their method of discretizing the integral equations does not allow the two-bound–one-free-magnon continuum to be distinguished from a true bound state.

Acknowledgments

This work was supported by the Natural Sciences and Engineering Research Council of Canada. Two of the authors (BWS) and (DAL) also acknowledge the support of NATO under Research Grant No 0087/87.

References

[1] Southern B W, Lee R J and Lavis D A 1994 *J. Phys.: Condens. Matter* **6** 10 075
[2] Lee R J 1992 Three magnon excitations in one dimensional quantum spin chains *MSc Thesis* University of Manitoba
[3] Southern B W, Liu T S and Lavis D A 1989 *Phys. Rev.* B **39** 12 160
[4] Bethe H A 1931 *Z. Phys.* **71** 205
[5] Sutherland B 1975 *Phys. Rev.* B **12** 3795
[6] Takhtajan L A 1982 *Phys. Lett.* **87A** 479
[7] Babujian H M 1982 *Phys. Lett.* **90A** 479
[8] Parkinson J B 1988 *J. Phys. C: Solid State Phys.* **21** 3793
[9] Batchelor M T and Barber M N 1990 *J. Phys. A: Math. Gen.* **23** L15

[10] Izyumov Yu A and Skryabin Yu N 1988 *Statistical Mechanics of Magnetically Ordered Systems* (New York: Plenum) pp 197–295
[11] Tsvelik A M 1990 *Phys. Rev.* **42** 779
[12] Grabowski M P and Mathieu P 1994 *Mod. Phys. Lett.* A **9** 2197
[13] Wortis M 1963 *Phys. Rev.* **132** 85
[14] Majumdar C K 1969 *J. Math. Phys.* **10** 177
[15] One I, Mikado S and Oguchi T 1971 *J. Phys. Soc. Japan* **30** 358
[16] Gochev I G 1973 *Theor. Math. Phys.* **15** 402
[17] Bahurmuz A A and Loly P D 1986 *J. Phys. C: Solid State Phys.* **19** 2241
[18] Tonegawa T and Harada I 1989 *J. Phys. Soc. Japan* **58** 2902
[19] Kadolkar C, Ghosh D K and Sarma C R 1992 *J. Phys.: Condens. Matter* **4** 9651
[20] Millet P J and Kaplan H 1974 *Phys. Rev.* B **10** 3923
[21] Cyr S L M 1994 Multi-magnon excitations in one-dimensional quantum spin chains with NNN interactions *MSc Thesis* University of Manitoba
[22] Lavis D A and Southern B W, unpublished
[23] Haydock R 1980 The recursive solution of the Schrödinger equation *Solid State Physics* vol 35 (New York: Academic) p 215
[24] Hodges C H 1977 *J. Physique Lett.* **38** L187
[25] Magnus A 1979 Recurrence coefficients for orthogonal polynomials on connected and non-connected sets *Padé Approximation and Its Applications; Proc. (Antwerp, 1979) (Springer Lecture Notes in Mathematics 765)* (Berlin: Springer)
[26] Turchi P, Ducastelle F and Tréglia G 1982 *J. Phys. C: Solid State Phys.* **15** 2891